

by Bernoullian statistics. At higher temperature, owing to steric hindrance, consecutive 1,2 placements are restricted ( $P_{a/a} \approx 0$ ) and the 1,2 units are no longer randomly distributed.

**Acknowledgments.** The authors thank the Canadian 220-MHz nmr Centre for making the nmr measurements. This work is supported by the National Research Council of Canada and the Quebec Ministry of Education.

## References and Notes

- (1) H. Yuki, Y. Okamoto, and H. Takano, *Polym. J.*, **2**, 663 (1971).
- (2) D. Blondin, J. Regis, and J. Prud'homme, *Macromolecules*, **7**, 187 (1974).
- (3) This model has been discussed in detail by F. A. Bovey, "High Resolution NMR of Macromolecules," Academic Press, New York, N. Y., 1972.

## Electrophoretic Light Scattering on Calf Thymus Deoxyribonucleic Acid and Tobacco Mosaic Virus

S. L. HARTFORD\*<sup>1</sup> and W. H. FLYGARE

Noyes Chemical Laboratory, University of Illinois, Urbana, Illinois 61801. Received June 24, 1974

Electrophoretic light scattering is a technique which combines electrophoresis with laser light-scattering spectroscopy.<sup>2</sup> In 1971, Ware and Flygare introduced electrophoretic light scattering by measuring the electrophoretic mobility of bovine serum albumin<sup>3</sup> and mobilities in mixtures of bovine serum albumin with fibrinogen.<sup>4</sup> Later, Uzgiris used this technique to measure the electrophoretic mobility of human erythrocytes, a bacterium (*Staphylococcus epidermidis*), and 0.357  $\mu$  polystyrene latex spheres.<sup>5</sup> Bennett and Uzgiris have also demonstrated the technique on 0.81  $\mu$  polystyrene latex spheres using a square wave AC field.<sup>6</sup> For further details, the reader is referred to views of the technique by Ware<sup>7</sup> and Flygare, Ware, and Hartford.<sup>8</sup>

Presently, electrophoretic light scattering has not been applied to systems of nucleic acids or viruses. We have applied this technique to the measurement of the electrophoretic mobility of calf thymus DNA and tobacco mosaic virus as a function of ionic strength. The results at high ionic strength are in agreement with measurements made using the Tiselius moving boundary electrophoresis technique.<sup>9-13</sup> Our measurements are reliably extended to low ionic strengths, and for TMV lower than any previous measurements. We find that the electrophoretic mobility is inversely proportional to the square root of the ionic strength at low ionic strength and approaches a constant value at higher ionic strength.

We have also measured the electrophoretic mobility of the denatured form of calf thymus DNA and have compared it to the native form. The mobilities obtained were  $u_{\text{native}}(20^\circ) = 5.0 \times 10^{-4} \text{ cm}^2 \text{ sec}^{-1} \text{ V}^{-1}$  and  $u_{\text{denatured}}(20^\circ) = 4.2 \times 10^{-4} \text{ cm}^2 \text{ sec}^{-1} \text{ V}^{-1}$  at 0.01 M NaCl and pH 7.0. These values and the approximately 15% difference between them agree with measurements made by the Tiselius technique.<sup>11,12</sup>

In addition, we have improved the design of the electrophoretic light-scattering cell invented by Ware and Flygare.<sup>14</sup> The improved design makes optical alignment of the cell much easier. Also the molecules in the scattering region are prevented from making direct contact with the electrodes.

## Theory

When an electric field is applied to charged molecules,

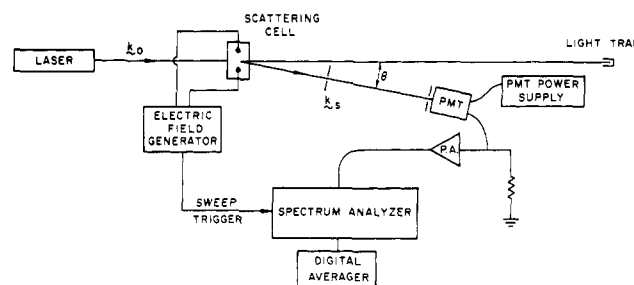


Figure 1. Block diagram of the experimental apparatus.

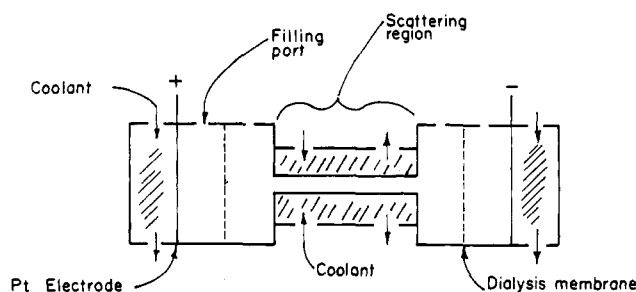


Figure 2. Cross-section of the electrophoretic light-scattering cell.

they will move in the direction of the electrode of opposite polarity. Laser light which is scattered from these molecules will be Doppler shifted. As the molecules migrate they also experience random Brownian motion which Doppler broadens the scattered light. The resulting spectrum is a Lorentzian shifted by a frequency proportional to the electrophoretic mobility with a half-width proportional to the translational diffusion coefficient. The theory has been worked out in detail by Flygare and Ware,<sup>3</sup> and we only summarize the result here. The heterodyne spectrum for the experimental geometry in Figure 1 is given by the equation

$$I(\omega) = NA^2 \left[ \frac{DK^2/\pi}{[\omega - \omega_0 + KuE \cos(\theta/2)]^2 + (DK^2)^2} \right]$$

where  $N$  is the number of molecules in the scattering region,  $A$  is an amplitude factor,  $E$  is the electric field (which is perpendicular to the incident radiation) applied to the molecules,  $D$  is the translational diffusion coefficient,  $\theta$  is the scattering angle,  $u$  is the electrophoretic mobility, and  $K$  is the scattering vector.  $K$  is equal to  $(4\pi n/\lambda_0) \sin(\theta/2)$  where  $n$  is the index of refraction of the medium and  $\lambda_0$  is the vacuum wavelength of the incident light.

The half-width at half-height of the Lorentzian spectrum is equal to  $DK^2/2\pi$ . The magnitude of the Doppler shift is equal to  $KuE \cos(\theta/2)/2\pi$ . Therefore, one can simultaneously measure the translational diffusion coefficient,  $D$ , and the electrophoretic mobility,  $u$ , from the spectrum.

## Experimental Section

Figure 1 is a diagram of the experimental apparatus. The laser source is a Spectra-Physics Model 165-03 argon-ion laser which is operated in a single mode of the 5145-Å resonance. Amplitude fluctuations in the laser are reduced by monitoring the output with a servo regulator which adjusts the power supply current to keep the intensity constant. The laser beam is focused into the electrophoretic light-scattering cell. The scattered light is collimated by pinholes and directed onto an RCA 7265 phototube. Enough light is scattered from the front window of the cell to serve as a local oscillator signal at the phototube. The signal from the phototube is preamplified by a Princeton Applied Research Model 113 preamplifier which is then the input into a Federal Scientific UA 15A

**Table I**  
**Electrophoretic Mobilities in Calf Thymus DNA**  
**and Tobacco Mosaic Virus as a Function**  
**of Ionic Strength**

Ionic strength	$u_{\text{DNA}}(20^\circ) \times 10^4$ $\text{cm}^2 \text{sec}^{-1} \text{V}^{-1}$	$u_{\text{TMV}}(20^\circ) \times 10^4$ $\text{cm}^2 \text{sec}^{-1} \text{V}^{-1}$
0.001		5.2
0.004	5.9	
0.01	5.0	3.5
0.02	4.4	2.7
0.05	3.3	1.9
0.10	2.8	1.5

real time spectrum analyzer. The spectra are stored and averaged in a Federal Scientific 1015 spectrum averager. The electrophoretic mobility is measured directly from the spectrum.

Figure 2 shows a cross-sectional diagram of the electrophoretic light-scattering cell. The laser beam is focused in the scattering region perpendicular to the plane of the diagram. The cell is simply aligned by directing the light reflected from the front and back windows of the scattering region back in the direction of the incident beam. Cells with scattering regions having heights of 2 and 4 mm have been used. In both cases the path length of the scattering region was 1 cm, making the cross-sectional area of the scattering regions 0.2 and 0.4  $\text{cm}^2$ , respectively. These dimensions allow effective cooling of the region. The temperature is monitored by means of a thermocouple. The dialysis membrane prevents molecules in the scattering region from coming in direct contact with the electrodes and also prevents any bubbles formed on the electrodes from entering the scattering region. The field is applied to the two platinum black electrodes.

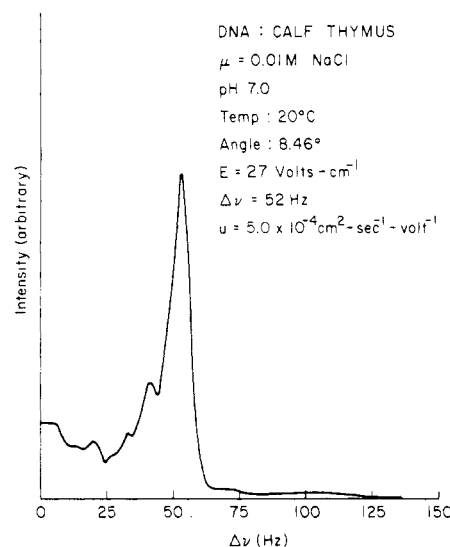
The electric field is applied in pulses of alternating polarity and duration of 0.1 to 1.0 sec. The electric field strength used in our experiments was between 0 and 100 V/cm. Concentration gradients are avoided by alternating the polarity of the pulses. After each pulse the field is turned off for a period equal to several pulse lengths so that the system has time to return to equilibrium. The pulse generator is synchronized with the spectrum analysis equipment so that data are accumulated only when the field is on.

Commercial calf thymus DNA Lot No. 82C-9500 Type I was purchased from Sigma Chemical Co. The DNA was phenol extracted<sup>15</sup> and exhaustively dialyzed to each ionic strength with NaCl at pH 7.0. Tobacco mosaic virus samples were provided by Dr. Russel Steere of the Department of Agriculture Plant Virological Laboratory at Beltsville, Maryland and Dr. Arthur Knight of the Biology Department at the University of California at Berkeley. The virus was dialyzed to each ionic strength used at pH 7.0. All samples were filtered through 0.8  $\mu$  millipore filters which had been pre-treated with a 0.1% solution of bovine serum albumin to prevent adsorption of the sample into the filter.<sup>16</sup>

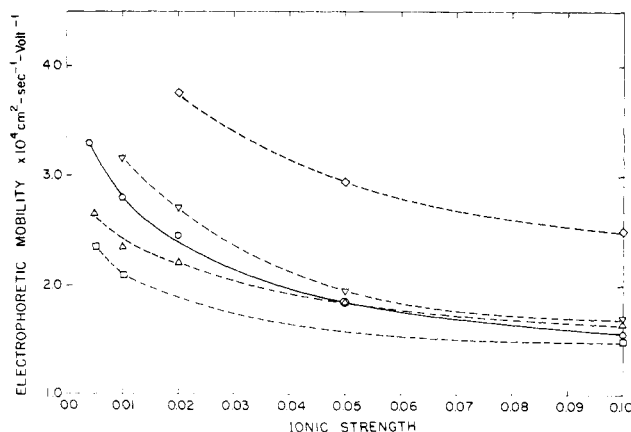
## Results and Discussion

Table I gives the values of the electrophoretic mobility obtained for calf thymus DNA and tobacco mosaic virus at each ionic strength. Figure 3, which is a typical electrophoretic light-scattering spectrum, is from a sample of DNA. The spectrum was signal averaged 100 times and took approximately 5 min to accumulate. The intensity at low frequency in the spectrum is probably the result of impurities in the sample or mechanical vibrations in our apparatus which modulate the laser intensity at low frequencies. Figures 4 and 5 are plots of the mobility of calf thymus DNA and tobacco mosaic virus, respectively, as a function of the ionic strength. Concentrations of calf thymus DNA were in the range 50–100  $\mu\text{g}/\text{ml}$  and in the range 0.1–0.5  $\text{mg}/\text{ml}$  for tobacco mosaic virus. Our measurements have a 5% standard deviation. Mobilities measured by other workers using the moving boundary technique are plotted for comparison.

For the calf thymus DNA the results are in agreement, within experimental error, for ionic strength greater than



**Figure 3.** Electrophoretic light-scattering spectrum of calf thymus DNA.



**Figure 4.** Mobility of calf thymus DNA plotted as a function of ionic strength: O, this work; ◇, ref 9; ▽, ref 10; Δ, ref 11; □, ref 12. (All data were viscosity corrected to 0°.)

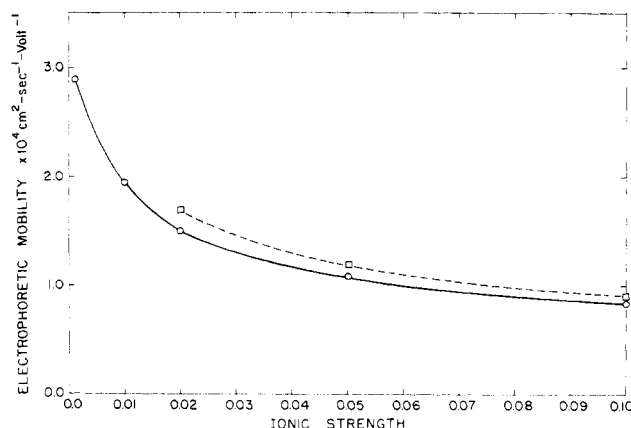


**Figure 5.** Mobility of tobacco mosaic virus plotted as a function of ionic strength: O, this work; □, ref 13. (All data were viscosity corrected to 0°.)

0.05 M NaCl (with the exception of the values from ref 9, where presumably some systematic error caused their data to be consistently high). The scatter in the moving boundary electrophoresis data at ionic strengths below 0.05 M NaCl indicates that the technique is less reliable at low ionic strengths. At low ionic strength the solution deviates significantly from Longworth's "ideal" conditions for elec-

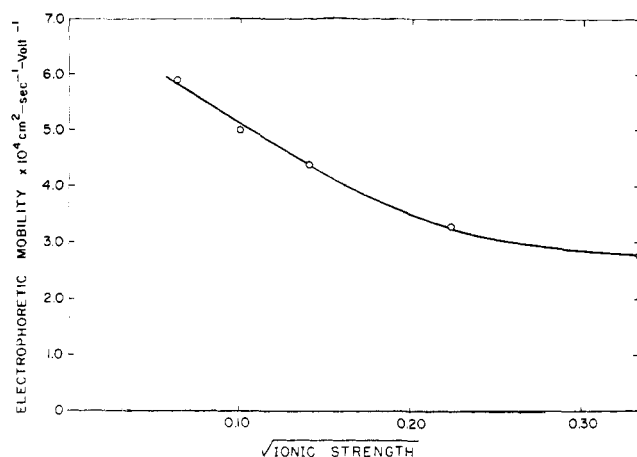


Figure 6. Mobility of calf thymus DNA at 20° plotted as a function of the square root of the ionic strength.

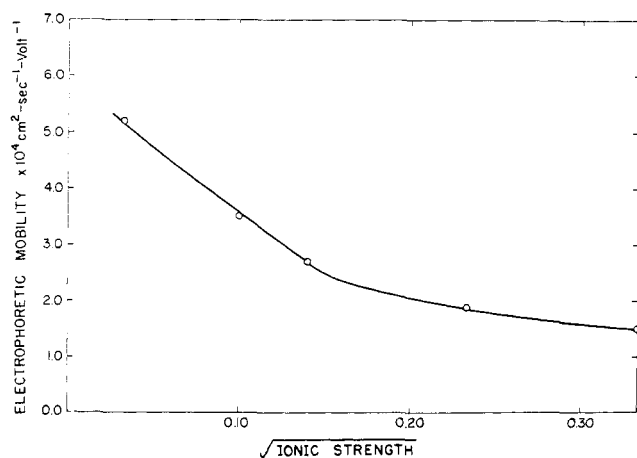


Figure 7. Mobility of tobacco mosaic virus at 20° plotted as a function of the square root of the ionic strength.

trophoresis which are very low macro-ion concentration and rather high ionic strength.<sup>17,18</sup> At low ionic strength the presence of the macro-ions makes a nonnegligible contribution to the properties of the solution and causes small gradients of conductivity, pH, and macro-ion concentration across the moving boundary which complicate the analysis of the data.

Conversely, low ionic strengths cause no problems in electrophoretic light scattering because the measurements are done at equilibrium and unstable concentration gradients are not formed in the solution. It is, in fact, advantageous to make electrophoretic light scattering measurements at low ionic strengths, because heating which causes convection is reduced. The heat developed in electrophoresis experiments is equal to  $H = E^2\kappa$ <sup>18</sup> where  $E$  is the electric field (in V/cm) and  $\kappa$  is the conductivity (in  $\text{ohm}^{-1}\text{cm}^{-1}$ ). Thus, lowering the conductivity, which is equivalent to lowering the ionic strength, will reduce the heating if the electric field remains constant. However, for our measurements on the calf thymus DNA, we restricted the ionic strength to values of 0.004 M NaCl and above, because the sample tends to denature if the ionic strength is made extremely low.<sup>11</sup>

For tobacco mosaic virus our results, within experimental error, are in agreement with previous results from the moving boundary electrophoresis technique.<sup>13</sup> In addition, we have extended our measurements to lower ionic strengths than were previously attainable for tobacco mosaic virus.

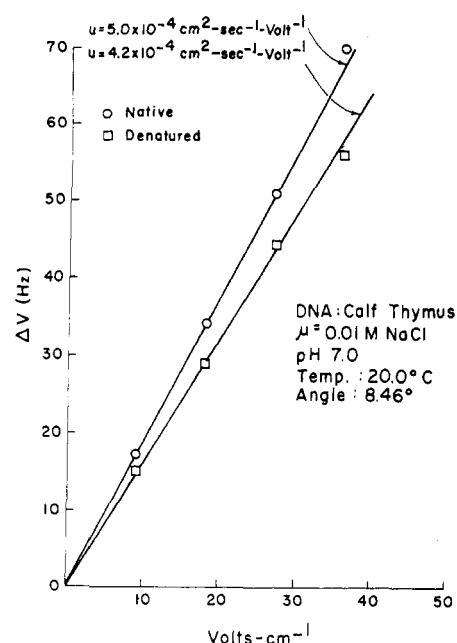


Figure 8. Electrophoretic frequency shifts as a function of electric field for the native and denatured forms of calf thymus DNA.

For both the calf thymus DNA and tobacco mosaic virus we did not attempt to measure the diffusion coefficient from the spectral line widths. Both samples were known to be very polydisperse making these measurements impractical.

Figures 6 and 7 are plots of the mobility of calf thymus DNA and tobacco mosaic virus, respectively, as a function of the square root of the ionic strength. In each case the mobility is linear in the square root of the ionic strength at low ionic strength, as predicted, and then approaches a constant value at higher ionic strength.<sup>19</sup>

We have also measured the electrophoretic mobility of the denatured form of calf thymus DNA at 0.1 M NaCl and pH 7.0. Denatured samples were prepared by immersing the native DNA in 95° water for 1 hr and then quickly transferring it to an ice bath for 10 min.<sup>12</sup> The electrophoretic mobility was then measured immediately.

Figure 8 shows a plot of the observed frequency shift as a function of the electric field strength. Each point is an average of several measurements and the graphs exhibit the predicted linear dependence with field strength. The measured values of the electrophoretic mobilities were

$$u_{\text{native}}(20^\circ) = 5.0 \times 10^{-4} \text{ cm}^2 \text{ sec}^{-1} \text{ V}^{-1}$$

$$u_{\text{denatured}}(20^\circ) = 4.2 \times 10^{-4} \text{ cm}^2 \text{ sec}^{-1} \text{ V}^{-1}$$

with a 5% standard deviation. When the data are viscosity corrected to 0°, it is in good agreement with electrophoretic mobilities measured with a conventional Tiselius electrophoresis cell.<sup>11</sup> The values obtained using the sucrose gradient electrophoresis apparatus<sup>12</sup> are lower than the others, but the percentage difference in mobility between the native and denatured form is in good agreement. Table II summarizes these data.

We have not observed the effects of electroosmosis<sup>20</sup> in our experiments. Electroosmosis occurs when oppositely charged particles in a capillary tube are attracted to the charged glass surface and move along the surface when an electric field is applied across the length of the tube. The particles moving along the glass surface cause a backflow of solution through the center of the tube which obscures the measurement of the electrophoretic mobility. We have

**Table II**  
Electrophoretic Mobilities in Native and Denatured Calf Thymus DNA

	$u_{\text{native}}(0^\circ) \times 10^4$ $\text{cm}^2 \text{sec}^{-1} \text{V}^{-1}$	$u_{\text{denatured}}(0^\circ) \times 10^4$ $\text{cm}^2 \text{sec}^{-1} \text{V}^{-1}$
This work	2.8	2.35
Ref 11	2.3	2.1
Ref 10	3.2	
Ref 12	2.17	1.90

used electrophoretic light scattering cells that have scattering regions with 0.2 and 0.4  $\text{cm}^2$  cross-sections and we have directed the laser light beam into different regions of the cross-sections, and in all cases we observe no changes in the frequency shifts (electrophoretic mobility). In addition, the frequency shifts are independent of preconditioning the cell with protein. Our consistent results agree with earlier conclusions on the negligible effects of electroosmosis.<sup>7,21</sup>

### Conclusion

Our measurements demonstrate that electrophoretic light scattering is well suited for measuring the electrophoretic mobilities of nucleic acids and viruses. This work and previous works<sup>3-5</sup> demonstrate that electrophoretic light scattering is a reliable way to measure electrophoretic mobilities from small proteins up to large bacteria. The technique has the following advantages over the conventional moving boundary technique: the technique is much faster; the experiment is done at equilibrium and does not require the build-up of unstable concentration gradients; instantaneous velocities are measured instead of long time migration of the molecules; the measurements can readily be done at higher temperatures, and measurements of lower ionic strengths can be made.

**Acknowledgment.** We acknowledge the work of I. Chabay in modifying the electrophoretic light-scattering cell. We would also like to thank Drs. Russel Steere and Arthur Knight for their generous samples of tobacco mosaic virus.

### References and Notes

- (1) NSF Predoctoral Trainee.
- (2) (a) H. Z. Cummins and H. L. Swinney, *Progr. Opt.*, **8**, 133 (1969); (b) G. B. Benedek, "Optical Mixing Spectroscopy, with Applications to Problems in Physics, Chemistry, Biology, and Engineering," "Polarisation Matière et Rayonnement, Livre de Jubilé in l'honneur du Professeur A. Kastler," Presses Universitaires de France, Paris, 1968, p. 49.
- (3) B. R. Ware and W. H. Flygare, *Chem. Phys. Lett.*, **12**, 81 (1971).
- (4) B. R. Ware and W. H. Flygare, *J. Colloid Interface Sci.*, **30**, 670 (1972).
- (5) E. E. Uzgiris, *Opt. Commun.*, **6**, 55 (1972).
- (6) A. J. Bennett and E. E. Uzgiris, *Phys. Rev. A*, **8**, 2662 (1973).
- (7) B. R. Ware, *Advan. Colloid Interface Sci.*, **4**, 1 (1974).
- (8) W. H. Flygare, B. R. Ware, and S. L. Hartford, "Electrophoretic Light Scattering," "Molecular Electro-Optics," C. T. O'Konski, Ed., Marcel Dekker, New York, N. Y., 1975.
- (9) A. R. Matheson and J. V. McLaren, *J. Chem. Soc.*, 303 (1956).
- (10) J. M. Creeth, D. O. Jordan, and J. M. Gulland, *J. Chem. Soc.*, 1406 (1949).
- (11) L. Constantino, A. M. Liquori, and V. Vitogliana, *Biopolymers*, **2**, 1 (1964).
- (12) B. M. Olivera, P. Baine, and N. Davidson, *Biopolymers*, **2**, 245 (1964).
- (13) I. Watanabe and N. Ui, *Bull. Chem. Soc. Jap.*, **29**, 345 (1956).
- (14) B. R. Ware, Ph.D. Thesis, University of Illinois, Urbana, Ill., 1972.
- (15) J. D. Mandell and A. D. Hershey, *Anal. Biochem.*, **1**, 66 (1960).
- (16) S. B. Dubin, J. H. Lunacek, and G. B. Benedek, *J. Mol. Biol.*, **54**, 547 (1970).
- (17) L. G. Longthorpe, *J. Phys. Colloid. Chem.*, **51**, 171 (1947).
- (18) R. A. Alberty, *J. Chem. Educ.*, **25**, 426, 619 (1948).
- (19) A. Tiselius and H. Svenson, *Trans. Faraday Soc.*, **36**, 16 (1940).
- (20) C. C. Brinton, Jr., and M. A. Lauffer, "Electrophoresis: Theory, Methods and Applications," Vol. I, M. Bier, Ed., Academic Press, New York, N. Y., 1964, p. 630.
- (21) H. A. Abramson, S. L. Mayer, and M. H. Goren, "Electrophoresis of Proteins," Reinhold, New York, N. Y., 1942.

### Reaction of Vinylidene Cyanide with Styrene. Structure of the Cycloadduct and Copolymer

J. K. STILLE\* and D. C. CHUNG

Department of Chemistry, University of Iowa, Iowa City, Iowa 52242. Received October 11, 1974

The reaction of vinylidene cyanide with styrene spontaneously yields an alternating copolymer and a product composed of one molecule of styrene and two molecules of vinylidene cyanide.<sup>1-5</sup> It has been suggested that the products arise from two competing reactions, although it was reported<sup>1</sup> that the trimer was formed only in the presence of large amounts of a free radical inhibitor, *tert*-butylhydroquinone. Oxidation of this trimer was also reported to yield phthalic acid, and 1-(2,2-dicyanoethyl)-4,4-dicyano-1,2,3,4-tetrahydronaphthalene was suggested as the structure of the product.

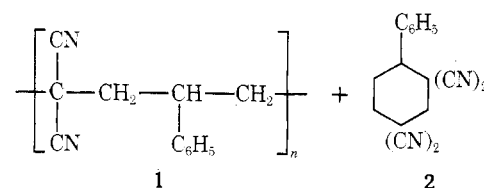
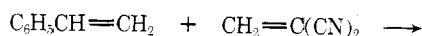
The reaction of styrene and vinylidene cyanide in benzene at 25° spontaneously yields an alternating copolymer (1) and the cycloadduct, 1,1,3,3-tetracyano-4-phenylcyclohexane (2) (Table I). The cycloadduct had the correct ele-

**Table I**  
Reaction of Vinylidene Cyanide (VC) with Styrene (ST) in Benzene at 25°

Molar ratio (VC/ST)	% yield <sup>a</sup>		$\eta_{sp}/c$ of copolymer <sup>b</sup>
	Cycloadduct	Copolymer	
2.17	20	78	0.45
1.45	23	53	0.65
0.73	33	49	0.57
0.47	30	53	0.69

<sup>a</sup> % yields were calculated with respect to the reactant present in the smaller molar amount. <sup>b</sup> Reduced viscosities were taken in dimethylformamide solutions, concentrations varying from 0.35 to 0.45 g/100 ml at 30°.

mental analysis and showed a parent ion in the mass spectrum,  $m/e$  260. Both the <sup>1</sup>H and <sup>13</sup>C nmr spectra were consistent with the assigned structure (Table II).



The copolymer was soluble in acetonitrile but insoluble in toluene. The composition of the copolymer was consistently 1:1, regardless of the feed ratio (Table III). The absence of <sup>13</sup>C absorption in the copolymer at 66.02 ppm corresponding to the C-2 of poly(vinylidene cyanide) and at 46 ppm corresponding to C-4 of polystyrene established the absence of blocks of polystyrene or poly(vinylidene cyanide) in the copolymer. The absence of absorption near 17.5 ppm excludes a head-to-head structure and supports the head-to-tail copolymer.

Thus, the closest intermediate, to both the cycloadduct and the copolymer, is perhaps a donor-acceptor complex since the cycloadduct is a product of a head-to-head addition of styrene and vinylidene cyanide, while the copolymer is head-to-tail.